

A monophasic extraction strategy for the simultaneous lipidome analysis of polar and nonpolar retina lipids[§]

Todd A. Lydic,* Julia V. Busik,[†] and Gavin E. Reid^{1,*§}

Departments of Chemistry,* Physiology,[†] and Biochemistry and Molecular Biology,[§] Michigan State University, East Lansing, MI 48824

Abstract Lipid extraction using a monophasic chloroform/methanol/water mixture, coupled with functional group selective derivatization and direct infusion nano-ESI-high-resolution/accurate MS, is shown to facilitate the simultaneous analysis of both highly polar and nonpolar lipids from a single retina lipid extract, including low abundance highly polar ganglioside lipids, nonpolar sphingolipids, and abundant glycerophospholipids. Quantitative comparison showed that the monophasic lipid extraction method yielded similar lipid distributions to those obtained from established “gold standard” biphasic lipid extraction methods known to enrich for either highly polar gangliosides or nonpolar lipids, respectively, with only modest relative ion suppression effects. This improved lipid extraction and analysis strategy therefore enables detailed lipidome analyses of lipid species across a broad range of polarities and abundances, from minimal amounts of biological samples and without need for multiple lipid class-specific extractions or chromatographic separation prior to analysis.—Lydic, T. A., J. V. Busik, and G. E. Reid. A monophasic extraction strategy for the simultaneous lipidome analysis of polar and nonpolar retina lipids. *J. Lipid Res.* 2014. 55: 1797–1809.

Supplementary key words lipidomics • lipid extraction • mass spectrometry • ganglioside • glycerolipid • sphingolipid

Lipids are multifunctional molecules that serve as the primary components of biological membranes, while also playing important roles in energy storage and signaling (1–3). Numerous perturbations of lipid metabolism and lipid signaling events have been identified as potentially important factors in the onset and progression of a diverse array of conditions including diabetes (4), cancer (5, 6), and Alzheimer’s disease (7). Recently, significant disruption of multiple lipid metabolic pathways including sphingolipid metabolism, fatty acid elongation and desaturation, and phospholipid metabolism have been associated with the development of several sight-threatening retinal pathologies

including diabetic retinopathy (8–12), Stargardt-like macular dystrophy (13), age-related macular degeneration (14), Smith-Lemli-Opitz syndrome (15), and retinopathy of prematurity (16). In some retinal disorders, particularly diabetic retinopathy, all of these metabolic defects may be present simultaneously (8–12). Unfortunately, analysis of structurally diverse lipid species such as sphingolipids, fatty acids, and phospholipids that span a wide range of polarities, degree of unsaturation, and abundance within a given tissue remains analytically prohibitive, particularly given the small amount of retinal tissue that may be obtained when using rodent models of retinal disease. Sphingolipid and glycerolipid metabolic and signaling pathways can generate highly polar lipid derivatives including gangliosides, ceramide (Cer)-1-phosphate, sphingosine-1-phosphate, and phosphorylated phosphatidylinositols (PIs), which typically cannot be extracted and utilized for lipid analysis together with the less polar lipid classes formed from these pathways (17–19). Clearly, given the importance of dysregulated lipid metabolism in a number of retinal disorders, studies aimed at elucidating the role of lipids in retinal diseases would benefit from analytical strategies capable of facilitating truly comprehensive lipid analysis of both polar and nonpolar lipid classes, as well as abundant and low abundance lipids, from a single lipid extract obtained from a minimal amount of a biological sample.

To address the growing need for robust lipid analysis platforms that facilitate a deeper understanding of lipid metabolism and lipid signaling networks (3, 20), MS based “lipidomics”, devoted to in-depth analysis of the lipid content of cells and tissues, has emerged as a subfield of systems biology. LC-MS has frequently been employed in lipidomic analyses, as the introduction of a chromatographic

Abbreviations: Cer, ceramide; DMBNHS, *S,S*-dimethylthiobutano ylhydroxysuccinimide ester; HCD, higher-energy collision-induced dissociation; nESI, nano-ESI; PA, phosphatidic acid; PC, phosphatidylcholine; PE, phosphatidylethanolamine; PG, phosphatidylglycerol; PI, phosphatidylinositol; PS, phosphatidylserine.

¹To whom correspondence should be addressed.

e-mail: reid@chemistry.msu.edu

[§]The online version of this article (available at <http://www.jlr.org>) contains supplementary data in the form of three figures.

This work was supported by funding from the National Institutes of Health to G.E.R. and J.V.B. (GM103508 and EY016077). The authors have no conflicts of interest to report.

Manuscript received 19 April 2014 and in revised form 29 May 2014.

Published, *JLR Papers in Press*, May 30, 2014

DOI 10.1194/jlr.D050302

separation step prior to MS or MS/MS enables excellent analytical specificity for a given lipid class (18, 21, 22). However, most LC-MS lipidomic methods are optimized for the separation and detection of only a few specific classes of structurally related lipids, thereby precluding global lipidome analysis from a single LC-MS run (23–26), increasing the required analytical time, sample usage, and potential introduction of experimental error.

Improved strategies for “shotgun” lipidomics, which involve the direct infusion of a lipid extract into a mass spectrometer without prior chromatographic separation steps (3), have enabled progressively broader “nontargeted” lipid analysis from milligram amounts of biological samples, often with greatly reduced analysis times relative to LC-MS (27–29). Traditionally, shotgun lipidomic studies have utilized triple quadrupole, ion trap, or hybrid high- and ultra high-resolution instruments to characterize numerous classes of lipids in a single analytical run, thereby providing a significant gain in analytical flexibility while providing similar or better sensitivity than LC-MS approaches, particularly when used in conjunction with nano-ESI (nESI) (30, 31). Despite these advantages, the majority of shotgun lipidomic strategies have enabled the profiling of a maximum of only a few hundred lipid species from a given cell or tissue extract (30, 32, 33). This is likely due to the combination of the limited dynamic ranges of the instruments employed in many of these studies, and the inability of mass spectrometers operating with unit mass resolution to resolve structurally distinct lipids which possess the same nominal mass, and that may yield similar product ions upon collision-induced dissociation (CID)-MS/MS. Moreover, detection of all molecular species within a given lipid class has proven to be problematic by traditional shotgun lipidomic approaches, particularly those presented with isobaric mass values. For example, plasmalogen (1-*O*-alkenyl ether) phospholipids exhibit isobaric overlap with 1-*O*-alkyl ether phospholipids (34), and are often under-detected by neutral loss or precursor ion scanning mode MS/MS experiments (35).

The recent application of high-resolution/accurate MS instrumentation to shotgun lipidomic analysis has facilitated the increasingly sensitive detection of lipid species across a large dynamic range in as little as a few minutes of acquisition time, greatly expanding lipidome coverage relative to other platforms (6, 32, 34, 36). Previously, we have shown that functional group-specific derivatization of phosphatidylethanolamine (PE) and phosphatidylserine (PS) aminophospholipids with a fixed charge sulfonium reagent, *S,S*-dimethylthiobutanoylhydroxysuccinimide ester (DMBNHS), further enables comprehensive lipidome analysis using high-resolution/accurate MS analysis strategies, via eliminating potential isobaric mass overlaps between these lipid classes and certain molecular species of phosphatidylcholine (PC), as well as ammonium-adducted phosphatidic acid (PA) and phosphatidylglycerol (PG) lipids (6, 34), while also increasing the sensitivity for detection of the derivatized lipid classes. Additionally, plasmalogen-specific functional group derivatization of the DMBNHS-labeled total lipid extracts with iodine and

methanol has been shown to resolve isobaric mass overlap between plasmalogen lipids and 1-*O*-alkyl ether-containing lipids (34). Together, these sequential lipid derivatization reactions overcome the isobaric overlap of lipid molecular species that has previously impeded comprehensive lipidome analysis by shotgun infusion high-resolution/accurate mass-based MS and/or MS/MS lipid identification approaches, and have been applied to the identification and characterization of >600 individual cellular lipids in cell culture models of colorectal cancer malignancy and metastasis (6). Therefore, shotgun lipidomic analysis strategies based on high-resolution/accurate mass platforms, in conjunction with functional group-specific lipid derivatization, have the potential to overcome existing analytical barriers to truly comprehensive lipidome coverage.

However, regardless of the platform selected for a given analysis, all lipidomic strategies first require the extraction of target lipids from their biological matrix. Lipid extraction from a given matrix is typically accomplished by the use of two-phase liquid/liquid extraction methods which partition hydrophobic lipids to an organic solvent phase, while unwanted proteins, nucleic acids, and cellular debris are partitioned to an interphase between the aqueous and organic phases (37–39). Unfortunately, lipid partitioning to the aqueous phase and/or losses to the interphase (and the subsequent introduction of experimental error) are inherent to biphasic lipid extraction strategies, particularly for species with relatively hydrophilic headgroups (such as gangliosides and lipid 1-phosphates) (18, 40), thereby limiting the scope of most “comprehensive” lipidomic studies. To circumvent this problem, a variety of specialized extraction methods have been specifically developed for several classes of hydrophilic lipids including gangliosides, phosphorylated PIs, and sphingolipid 1-phosphates (17–19, 41). Therefore, comprehensive lipidomic studies that aim to examine both polar and nonpolar lipid analytes typically require several specialized types of lipid extractions from the same matrix (32), which may introduce additional experimental errors and increased sample preparation and analysis times, or may not be feasible from limited amounts of tissues or cells.

Gangliosides exemplify a lipid class that typically requires specialized lipid extraction methods, and thus poses a significant obstacle to the goal of achieving truly comprehensive analysis of all lipid species present in a biological sample (17). While brain homogenates have typically been utilized for the development of methods for the analysis of these sialic acid-bearing polar sphingolipids, the limited yield of retinal tissue that can be obtained from animal models has, to date, prevented in-depth lipidomic analysis of retinal ganglioside compositions. However, gangliosides are known to participate in a number of biological processes which may be relevant to retinal physiology, as well as vision disorders involving loss of photoreceptors or pathological retinal neovascularization. For example, gangliosides have been shown to modulate axonal growth (42), apoptosis (43, 44), vascular endothelial growth factor receptor function, angiogenic signaling (40, 45, 46), insulin signaling (47), and the binding of leukocytes to endothelial cells (48).

Numerous lipidomic methods for the characterization of gangliosides obtained from polar lipid extracts have been developed based on LC-MS platforms (23, 49) as well as direct infusion by nESI (50, 51), including the use of the high-resolution/accurate mass Orbitrap platform (52). However, all ganglioside analysis methods reported to date have involved either the initial extraction and specific enrichment of gangliosides at the exclusion of other lipid classes by using variants of the classical Svennerholm ganglioside extraction method (17) or via the fractionation of total lipid extracts by chromatographic separation.

To facilitate future studies of retinal lipid metabolism in sight-threatening vision disorders that require the comprehensive analysis of structurally distinct subsets of the lipidome, we sought to define a lipidomic strategy capable of bridging the analysis of relatively low abundance polar lipids, such as gangliosides, with nonpolar sphingolipids and abundant polar and nonpolar glycerolipids from a small amount of available biological tissue, such as a single rat retina.

MATERIALS AND METHODS

Materials

Isopropanol, methanol, and water were purchased from J.T. Baker (Phillipsburg, NJ). Chloroform was from EMD Chemicals (Billerica, MA). All solvents used were high-performance LC grade. Ammonium formate was purchased from Alfa Aesar (Ward Hill, MA). Standard lipids, PC_(14:0/14:0), PE_(14:0/14:0), and PS_(14:0/14:0), were purchased from Avanti Polar Lipids (Alabaster, AL). Ganglioside lipid standards were purchased from Matreya (Pleasant Gap, PA). All lipid extraction solvents contained 0.01% butylated hydroxytoluene from Sigma Aldrich (St. Louis, MO).

Animals

Male BBDR/Wor rats were obtained from Biomedical Research Models (Worcester, MA) and maintained on standard rodent diet AIN-93M from Dyets Inc. (Bethlehem, PA) until 191–194 days old. Immediately prior to retina isolation, rats were euthanized under anesthesia (isoflurane/Vapomatic) by heart puncture and exsanguination. To obtain retinas, eyes were enucleated and rinsed in ice-cold PBS, opened by a circumferential incision just below the ora serrata, and the anterior segment and vitreous were discarded. Retinas were then lifted off the eyecup, weighed, snap-frozen in liquid nitrogen, and maintained at -80°C until use. All procedures involving the animals adhered to the Association for Research in Vision and Ophthalmology statement for the use of animals in ophthalmic and vision research. The protocols for the animal studies were approved by the Institutional Animal Care and Use Committee at Michigan State University.

Tissue homogenization

Three frozen retinas (approximately 15 mg each) obtained from separate animals were suspended in ice-cold 40% methanol (50 μl /mg retina tissue) (53). Samples were homogenized for 5 min using 0.5 mm zirconium oxide beads in an air-cooled Bullet blender (Next Advance, Averill Park, NY), and homogenates were pooled and mixed thoroughly. Nine aliquots of the pooled retina homogenate, corresponding to 5 mg tissue equivalents in

a volume of 250 μl each, were then transferred to glass tubes for subsequent lipid extraction by three different methods (each in triplicate) as outlined below.

Modified Svennerholm lipid extraction

One set of three aliquots of retina tissue homogenate was subjected to biphasic lipid extraction based on a modified version of the Svennerholm method (17) as reported by Fong et al. (49). To each of the three 5 mg aliquots of retina tissue homogenate, methanol (1.25 ml), chloroform (0.675 ml), and water (0.35 ml) were added to create a monophasic extraction mixture with a final ratio of 2:1:0.74 (v:v:v) methanol/chloroform/water, including water and methanol present in the retina homogenate. Samples were vortexed for 1 min, and then incubated at room temperature for 30 min with shaking. Extracts were then centrifuged at 2,000 *g* for 30 min at room temperature to precipitate proteins, and the supernatants were collected. Protein pellets were then resuspended in water (0.25 ml) by vortexing, and re-extracted with chloroform/methanol (1:2, v:v, 1.0 ml) by incubation and centrifugation as described above. The supernatants from the repetitive extractions were collected and pooled, and the pellets were discarded. This monophasic lipid extract was then subjected to phase separation to create a ganglioside-enriched upper phase by the addition of 0.65 ml water, followed by incubation at room temperature for 30 min with shaking, then centrifugation for 30 min at 2,000 *g*. The upper phase was collected, and the lower phase and interphase were re-extracted with 0.25 ml of 0.01 M KCl to facilitate precipitation of the remaining proteins. The samples were incubated and centrifuged as before, and the upper aqueous phases from the repetitive extractions were pooled, generating a polar lipid extract enriched in gangliosides and depleted of phospholipids. Both the polar upper phase and nonpolar lower phase were dried under nitrogen then resuspended in isopropanol/methanol/chloroform (4:2:1, v:v:v) (6, 9) at a concentration of 20 mg/ml retina tissue extracted. Reconstituted retina lipid extracts were centrifuged at 2,000 *g* to remove any residual particulates, then transferred to 2.0 ml glass vials and stored at -80°C until further use. Initial investigations indicated the polar lipid extract was suitable for ganglioside analysis without the introduction of further phase partitioning, desalting, or other sample cleanup steps when analyzed under the conditions described below. Using this method, a total of three replicate polar upper phase and three replicate nonpolar lower phase retina lipid extracts were obtained, each derived from 5 mg of retina tissue (corresponding to one third of a single retina).

Modified Folch lipid extraction

A second set of three aliquots of retina tissue homogenate were subjected to biphasic lipid extraction by a modified Folch procedure using four volumes (1.0 ml) of chloroform/methanol (2:1, v:v) (53) by incubating samples at room temperature for 30 min with shaking, followed by centrifugation at 2,000 *g* for 30 min at room temperature, and re-extraction of the aqueous phase with 1.0 ml of 100% chloroform. Both the aqueous upper phase (enriched in polar lipids and metabolites) and the organic lower phase (enriched in phospholipids and neutral lipids) were collected separately, and organic lower phases from the repetitive extractions were pooled. Lipid extracts were dried under nitrogen then resuspended in isopropanol/methanol/chloroform (4:2:1, v:v:v) at a concentration of 20 mg/ml retina tissue extracted. Reconstituted retina lipid extracts were centrifuged at 2,000 *g* to remove any residual particulates, then transferred to 2.0 ml glass vials and stored at -80°C until further use. Using this method, a total of three replicate polar upper phase and three replicate nonpolar lower phase retina lipid extracts were obtained,

each derived from 5 mg of retina tissue (corresponding to one-third of a single retina).

Monophasic lipid extraction

The remaining set of three aliquots of retina tissue homogenates was subjected to monophasic methanol/chloroform/water lipid extraction exactly as described above for the initial steps of the modified Svennerholm lipid extraction, including re-extraction of the protein pellet. However, after pooling the monophasic supernatants from repetitive extractions of the retina homogenate, no phase separation was induced, and the monophasic lipid extracts containing both polar and nonpolar lipids were immediately dried under nitrogen and resuspended in isopropanol/methanol/chloroform (4:2:1, v:v:v) at a concentration of 20 mg/ml retina tissue extracted. Reconstituted retina lipid extracts were centrifuged at 2,000 *g* to remove any residual particulates, then transferred to 2.0 ml glass vials and stored at -80°C until further use. Using this method, a total of three replicate monophasic retina lipid extracts were obtained, each derived from 5 mg of retina tissue (corresponding to one-third of a single retina).

Sequential functional group-specific derivatization and high-resolution/accurate MS analysis

Prior to MS analysis in positive ionization mode, half of each retina lipid extract from each of the above extraction methods was subjected to sequential functional group selective modification of: *i*) amine-containing PE and PS lipids using $^{13}\text{C}_1$ -DMBNHS; and *ii*) the *O*-alkenyl ether double bond of plasmalogen lipids using iodine and methanol, as previously described (34). The samples were then washed twice with 10 mM ammonium bicarbonate to remove excess salts and derivatization reagents. Forty microliters of reconstituted, derivatized (for positive ionization mode analysis), or nonderivatized (for negative ionization mode analysis) lipid samples were then transferred into individual wells of a Whatman Multi-Chem 96-well plate (Sigma Aldrich) and dried under nitrogen. Immediately before analysis, lipid extracts were resuspended in isopropanol:methanol:chloroform (4:2:1, v:v:v) containing 20 mM ammonium formate and $\text{PC}_{(14:0/14:0)}$ as an internal standard, unless otherwise noted. Sample dilutions and concentrations of internal standards are described in the Results section below. Samples were sealed with Teflon Ultra Thin sealing tape (Analytical Sales and Services, Pompton Plains, NJ), and 10 μl of each sample was aspirated and introduced to a high-resolution/accurate mass Thermo Scientific model LTQ Orbitrap Velos mass spectrometer (San Jose, CA) using an Advion Triversa Nanomate nESI source (Advion, Ithaca, NY) with a spray voltage of 1.4 kV and a gas pressure of 0.3 psi. The ion source interface settings (inlet temperature of 100°C and S-lens value of 50%) were optimized to maximize the sensitivity of the precursor ions while minimizing "in-source" fragmentation. High-resolution mass spectra, signal averaged for 2 min over the *m/z* range 200–2,000, were acquired in positive ionization mode using the fourier transform analyzer operating at 100,000 mass resolving power.

High-resolution mass spectra were also acquired in negative ionization mode from the underivatized lipid extracts, and signal averaged for 2 min over the *m/z* range 200–2,000. Where applicable, positive and negative ionization mode higher-energy collision-induced dissociation (HCD)-MS/MS product ion spectra were also acquired from monoisotopically isolated precursor ions from the underivatized lipid extracts (100,000 mass resolving power), to confirm phospholipid and ganglioside lipid assignments. HCD-MS/MS collision energies were individually optimized for each lipid class of interest using commercially available lipid standards when available.

Peak finding, lipid identification, and quantification

Initial lipid identifications were achieved using the lipid mass spectrum analysis (LIMSA v.1.0) software linear fit algorithm, in conjunction with a user-defined database of hypothetical lipid compounds for automated peak finding and correction of ^{13}C isotope effects. Quantification of the abundances of lipid molecular species between samples was performed by normalization of target lipid ion peak areas to the $\text{PC}_{(14:0/14:0)}$ internal standard (6). Identified lipids are reported only at the sum composition level (i.e., head group and fatty acyl or sphingosyl total carbons:double bonds), as the level of molecular detail (i.e., precise acyl chain compositions) determined by HCD-MS/MS was not required to demonstrate that the various lipids of interest were detected at similar relative abundances using the different extraction methods. Due to the lack of available lipid standards representing individual molecular species of gangliosides and many other lipid classes typically analyzed in lipidomics experiments, no attempts were made to quantitatively correct for different ESI responses of individual lipid species due to concentration, acyl chain length, or degree of unsaturation. Therefore, the abundances of lipid molecular species is reported only as the percentage of the total lipid ion abundance [after normalization against the $\text{PC}_{(14:0/14:0)}$ internal standard] for each lipid class, and are not intended to represent absolute concentrations of each lipid species.

Statistical analysis

Sample means of lipid molecular species, relative levels of lipid classes, and detector response as a function of sample concentration were analyzed for statistical significance by ANOVA followed by Sidak's multiple comparisons test using GraphPad Prism version 6.0 software. Sample means of summed ion abundances were analyzed for statistical significance by Student's *t*-test. Statistical significance was set at $P < 0.05$.

RESULTS AND DISCUSSION

Comparison of high-resolution/accurate mass spectra obtained from biphasic and monophasic retina lipid extracts

Prior to evaluating the utility of the monophasic extraction protocol for the simultaneous analysis of both polar and nonpolar lipid classes present across a wide range of abundances, we first evaluated two well established gold standard biphasic lipid extraction techniques for the selective extraction and enrichment of highly polar (e.g., gangliosides) and nonpolar lipids, respectively. Ganglioside lipid analysis procedures typically consist of an initial step involving the extraction of lipid classes from a given tissue, followed by one or more phase partitioning steps to subsequently remove most nonpolar lipid classes (17, 49). Conversely, biphasic extraction procedures used for the isolation of phospholipids and other nonpolar lipids lead to their nearly complete partitioning in an organic phase, while polar lipids such as gangliosides may equilibrate between the organic and aqueous phases.

As described above, methanol/water homogenates of BBDR/Wor rat retinas were split into three aliquots containing equivalent amounts of tissue (each corresponding to approximately 5 mg of retina) in equivalent volumes.

Then, two aliquots of retina tissue were subjected to biphasic lipid extraction using either the modified Svennerholm (49) or Folch methods. A third aliquot of retina homogenate was extracted using only a monophasic methanol/chloroform/water mixture identical to that used in the initial step of the modified Svennerholm extraction method, but without further induction of phase separation. Aliquots of the upper and lower phases from both biphasic extraction methods and the monophasic extract were then subjected to nESI-high-resolution/accurate mass analysis.

Figure 1A shows the negative ionization mode mass spectrum acquired from the upper (aqueous) phase of the ganglioside-enriched modified Svennerholm retina lipid extract, at a sample concentration corresponding to 1.0 mg/ml of original retina tissue extracted. Based on accurate mass measurements and the observed isotopic distributions, several ions were assigned as doubly deprotonated putative species of di- and tri-sialated gangliosides, including GD3_(36:1) at m/z 734.9128, GD1_(36:1) at m/z 917.4791, and GT1_(36:1) at m/z 1,063.0264. Good agreement between measured and theoretical masses was observed. For example, GD3_(36:1) and GD3_(38:1) were both observed within 0.0002 m/z of their theoretical values of 734.9126 and 748.9283, respectively.

Figure 1B shows the negative ion mass spectrum obtained over an equivalent m/z range from the lower (organic) phase of the modified Svennerholm retina lipid extract.

As expected, MS analysis of this lipid extract revealed many $[M-H]^-$ and $[M+HCO_2]^-$ ions corresponding to phospholipid species, in good agreement with our previous analyses of retina phospholipid content. For example, accurate mass measurements indicated that the abundant ions at m/z 790.5389 and 878.5915 in Fig. 1B corresponded to PE_(40:6) and the $[M+HCO_2]^-$ adduct of PC_(40:6), respectively. A comparison of the insets in Fig. 1A, B demonstrate that the lower phase of the modified Svennerholm lipid extract is essentially devoid of the putative retinal gangliosides, GD3_(36:1) and GD3_(38:1), seen in the aqueous upper phase extract, indicating effective partitioning of these polar ganglioside lipids into the aqueous upper phase. Conversely, while most phospholipids were effectively partitioned into the organic lower phase of the modified Svennerholm lipid extract, several species, including the relatively polar phospholipids PS_(40:6) at m/z 834.5293 and PI_(38:4) at m/z 885.5498, were observed primarily in the upper phase of the modified Svennerholm lipid extract. However, a trace amount of PI_(38:4) was also observed in the lower phase in Fig. 1B, indicating differential partitioning of this phospholipid class between the two phases as a function of the head group identity.

While the aqueous phases of other standard biphasic lipid extraction procedures, such as the modified Folch lipid extraction method, have also been previously reported for the analysis of polar lipid species such as gangliosides (40), we determined here that retina gangliosides

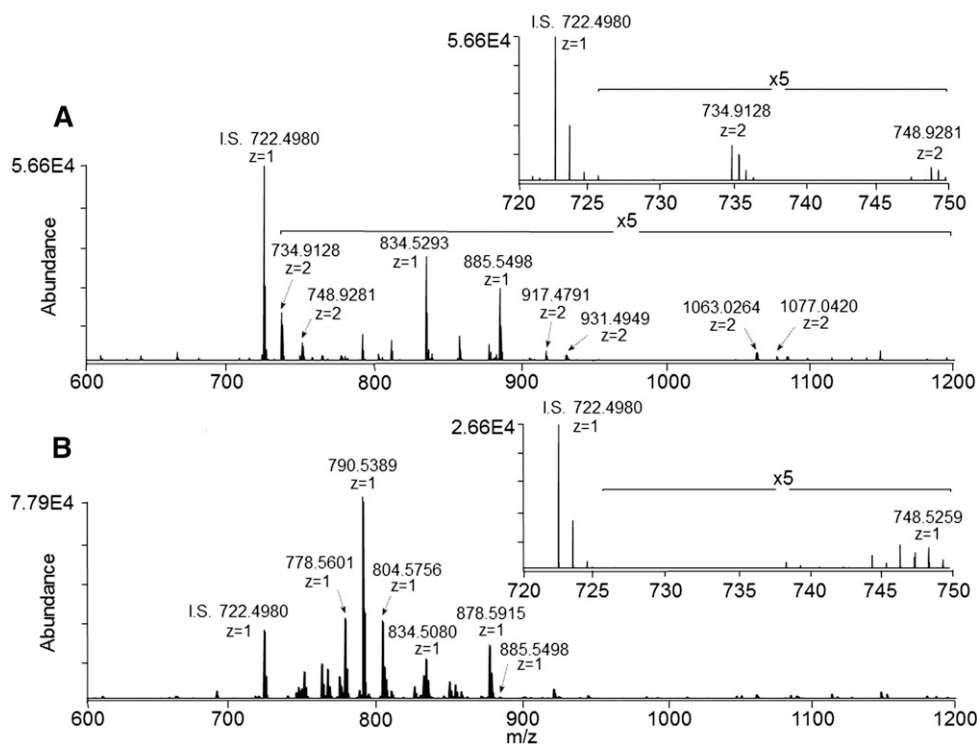


Fig. 1. A: Negative ionization mode high-resolution ($R = 100,000$)/accurate mass spectrum of a ganglioside-enriched modified Svennerholm upper phase retina lipid extract (sample concentration corresponding to 1.0 mg/ml of original retina tissue extracted). Inset: expanded region of the mass spectrum from m/z 720 to 750 showing doubly deprotonated ganglioside GD3 species. B: Negative ionization mode high-resolution ($R = 100,000$)/accurate mass spectrum of the modified Svennerholm lower phase retina lipid extract. Inset: expanded region of the mass spectrum from m/z 720 to 750. I.S., internal standard. PC_(14:0/14:0) (0.5 μ M).

were distributed approximately in a 1:1 ratio between the upper and lower Folch extraction phases (see supplementary Fig. 1A and supplementary Fig. 1B, respectively), thereby rendering ganglioside analysis impractical by using this extraction method.

Figure 2 shows the mass spectrum obtained from the monophasic retina lipid extract, which must contain both the polar lipid classes, such as gangliosides observed in Fig. 1A, and the nonpolar lipid classes observed in Fig. 1B, given that the modified Svennerholm upper and lower phases were derived from this initial monophasic extract. Notably, this monophasic retina lipid extract contains the same abundant phospholipid species as observed in Fig. 1B, while exhibiting increased levels of PS_(40:6) and PI_(38:4) relative to the modified Svennerholm lower phase in Fig. 1B due to the elimination of partitioning of these species to the upper phase. Additionally, the inset in Fig. 2 demonstrates the presence of the same retina gangliosides, GD3_(36:1) and GD3_(38:1), that were observed in the modified Svennerholm upper phase extract in Fig. 1A. This data suggests that the monophasic retina lipid extraction procedure may provide for the simultaneous analysis of both polar and nonpolar lipid classes within a single mass spectrum.

Evaluation of absolute and relative ion suppression effects as a function of sample dilution

To determine the extent to which the presence of abundant phospholipid ions in the monophasic retina lipid extract may inhibit the detection of lower abundance ions (54, 55) such as gangliosides, we next measured and compared the detector response for selected ions in both the modified Svennerholm upper phase and the monophasic retina lipid extracts. Three replicate extracts obtained by each extraction method (sample concentrations corresponding to 20.0 mg/ml of original retina tissue extracted) were spiked with 10 pmol/μl of PC_(14:0/14:0) as an internal standard, then subjected to serial dilution to yield extracts corresponding to concentrations within the range from 4.0 mg/ml to 0.125 mg/ml of retinal tissue equivalents.

Each extract was then analyzed by negative ionization mode nESI-high-resolution/accurate mass MS, and the mean ion abundance was determined for the ion at m/z 734.9128 [corresponding to ganglioside GD3_(36:1)], as well as for the ion at m/z 722.4980 corresponding to the $[M+HCO_2]^-$ adduct of the PC_(14:0/14:0) internal standard. A plot of ion abundance for m/z 734.9128 as a function of sample concentration for both the modified Svennerholm upper phase (open diamonds) and the monophasic (closed squares) extracts are shown in **Fig. 3A**. Significant ion suppression of m/z 734.9128 was observed for both extracts at higher sample concentrations ranging from 20 mg/ml to 2 mg/ml retinal tissue equivalents, as evidenced by the nonlinearity of ion abundance with sample concentration over this range. Additionally, the suppression effect was found to be greater in the monophasic lipid extract than in the modified Svennerholm upper phase extract, as evidenced by the lower absolute ion abundance of m/z 734.9128 in the monophasic compared with the upper phase extract. This effect is most likely due to the higher total lipid concentration within the monophasic lipid extract resulting in a lack of sufficient charge within the electrospray droplet to facilitate the ionization of these low abundance ions, relative to the less complex mixture in the modified Svennerholm upper phase lipid extract (55).

However, closer examination of the ion abundance for the GD3_(36:1) lipid at sample concentrations ranging from 1 mg/ml to 0.125 mg/ml for both the monophasic and modified Svennerholm upper phase lipid extracts (Fig. 3B) revealed a linear relationship between sample concentration and ion abundance. Moreover, the observed differences in absolute ion abundance between the two extracts were minimized at the lowest concentrations examined, albeit with a concomitant significant decrease in sensitivity. Notably, the ion abundance for m/z 734.9128 in the modified Svennerholm upper phase lipid extract was associated with increased experimental error relative to the monophasic extract, as evidenced by the larger standard deviations for the upper phase extract shown in Fig. 3A, B. This effect is most likely

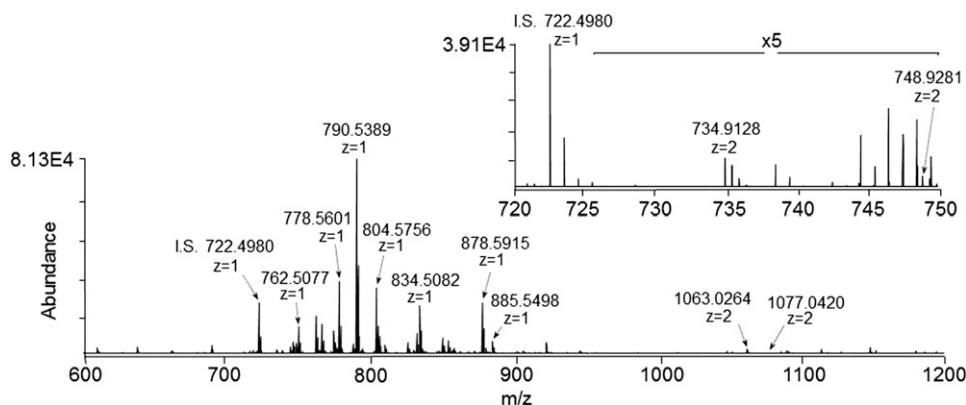


Fig. 2. Negative ionization mode high-resolution ($R = 100,000$)/accurate mass spectrum of a monophasic retina lipid extract (sample concentration corresponding to 1.0 mg/ml of original retina tissue extracted). Inset: expanded region of the mass spectrum from m/z 720 to 750 showing doubly deprotonated ganglioside GD3 species. I.S., internal standard. PC_(14:0/14:0) (0.5 μM).

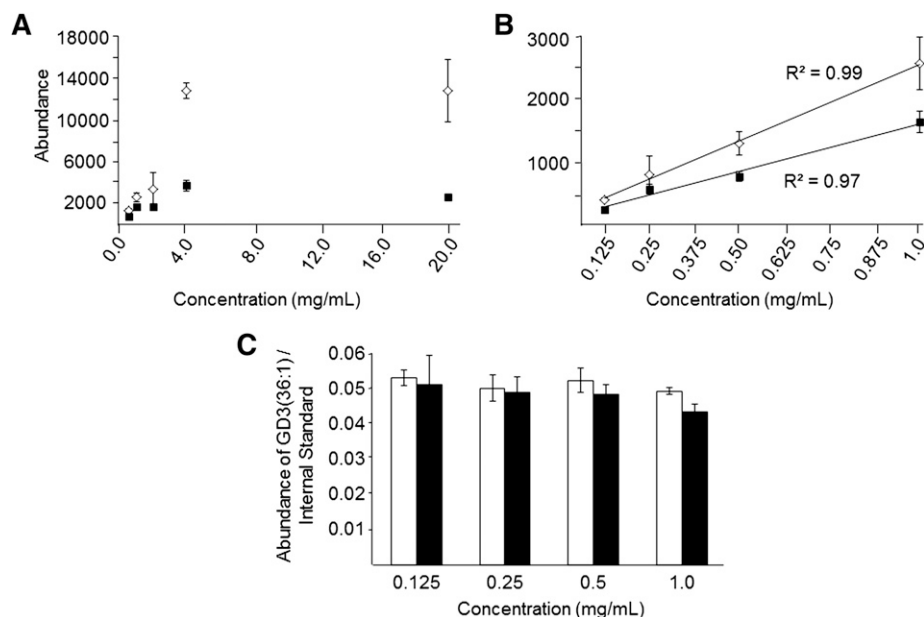


Fig. 3. Absolute ion suppression of ganglioside $\text{GD3}_{(36:1)}$ ions at m/z 734.9128 as a function of sample concentration measured by negative ionization mode high-resolution ($R = 100,000$)/accurate MS from modified Svennerholm upper phase retina lipid extracts (open diamonds) and monophasic lipid extracts (filled squares). Serial dilution of each lipid extract was performed from 20 mg/ml (retina tissue extracted/volume of lipid extract) to 0.5 mg/ml (A), and from 1.0 mg/ml to 0.125 mg/ml (B) where the abundance of m/z 734.9128 was observed to follow a linear dependence with retina lipid extract concentration from each extraction method. C: Comparison of relative ion suppression of ganglioside $\text{GD3}_{(36:1)}$ at m/z 734.9128, determined as the ratio of the absolute abundance of ganglioside $\text{GD3}_{(36:1)}$ to the absolute abundance of a $\text{PC}_{(14:0/14:0)}$ internal standard $[\text{M}+\text{HCO}_2]^-$ ion at m/z 722.4980, from the modified Svennerholm (open bars) and monophasic (filled bars) lipid extracts at each sample concentration within the linear range shown in (B). Data represent the mean \pm standard deviation from $n = 3$ separate lipid extracts.

due to the greater variation associated with complete removal and collection of the upper phase in the modified Svennerholm lipid extraction method, compared with the monophasic lipid extraction approach where no separate phase collection step was required. Essentially identical ion suppression effects were also observed for the $\text{PC}_{(14:0/14:0)}$ internal standard (see supplementary Fig. IIA, B). Note that ion suppression may be considered as being either “absolute”, i.e., as evidenced by nonlinearity of absolute ion abundance for an ion of interest as a function of increasing concentration (as described above), or “relative”, i.e., as evidenced by a decrease in the ratio of the abundance of an ion of interest compared with an internal standard as a function of increasing concentration. Therefore, we next calculated the ratio of the abundance of the $\text{GD3}_{(36:1)}$ lipid to the $\text{PC}_{(14:0/14:0)}$ internal standard within the linear concentration range of detector response for each ion (i.e., 1.0–0.125 mg/ml retina tissue extracted). Graphs comparing these ratios for both the modified Svennerholm upper phase and monophasic lipid extracts are shown in Fig. 3C. At the highest sample concentration in Fig. 3C, the ion abundance ratio of $\text{GD3}_{(36:1)}/\text{PC}_{(14:0/14:0)}$ in the monophasic extract was found to be 12% lower than that of the modified Svennerholm upper phase extract. A difference of 7.5% was also observed at a concentration of 0.5 mg/ml, although these modest differences did not reach the level of statistical significance at either sample concentration. The ratios at 0.25 and 0.125 mg/ml sample concentrations were essentially

identical from both extraction methods. A similar result was obtained for the most abundant phospholipid ion observed in the mass spectrum of the monophasic lipid extract in Fig. 2, namely $\text{PE}_{(40:6)}$ at m/z 790.5389, where the ratio of the absolute abundance of this ion to the absolute abundance of the internal standard did not change significantly over the entire 1.0–0.125 mg/ml sample concentration range (see supplementary Fig. IIC).

These results indicate that relative ion suppression effects are minimized when operating within the linear concentration range of detector response for a given ion, even when absolute ion suppression is observed. Furthermore, both relative and absolute ion suppression effects can be essentially eliminated by adequate dilution of the sample. However, the concomitant decrease in absolute ion abundance (and therefore sensitivity), and the increase in error associated with making ion abundance measurements at the lower sample concentrations required for elimination of all ion suppression effects (see supplementary Fig. III and the discussion below), makes this approach impractical for the measurement and quantification of very low abundance lipid species.

Evaluation of retina ganglioside profiles from monophasic versus modified Svennerholm upper phase lipid extracts

Given the modest relative ion suppression observed for the $\text{GD3}_{(36:1)}$ lipid at the highest sample concentration for

which a linear range of detector response was observed (i.e., 1 mg/ml), we next sought to determine the practical implications of any observed absolute and relative ion suppression effects in the monophasic lipid extract, relative to the modified Svennerholm upper phase extract, by performing a thorough analysis of the low-abundance GM3, GD1, GD3, GT1, and GQ1 retinal gangliosides observed within each extract at this sample concentration. Other ganglioside lipid classes, including GM1, GM2, GD2, GT2, and GP, were not observed in this study above the limits of detection using either retina tissue extraction method. In order to confirm the putative retina ganglioside species identified by accurate mass measurements, negative ionization mode HCD-MS/MS was utilized to detect the presence of characteristic ganglioside product ions in both the modified Svennerholm upper phase and monophasic retina lipid extracts, as previously described (56), and by comparison to HCD-MS/MS results obtained from commercially available ganglioside standards. As shown in Fig. 4A, the relative distributions of retina ganglioside lipid subclasses identified in both lipid extraction protocols were strikingly similar. These results reveal that retina is enriched primarily in the di- and tri-sialo gangliosides, GD1, GD3, and GT1, with GD3 species, comprising the majority of all retina ganglioside species. Low levels of

gangliosides containing one (GM3) and four (GQ1) sialic acids were also detected. Similarly, the relative distributions of individual ganglioside species within a particular lipid class were also very comparable between the two lipid extraction methods, as exemplified by the relative abundances of individual GD3 retina lipid species shown in Fig. 4B. Only one species, GD3_(34:1), exhibited a statistically significant, albeit modest, difference in relative abundance between the two extraction methods.

The sum of the abundances of all retinal ganglioside species normalized to the abundance of the PC_(14:0/14:0) internal standard, expressed relative to the modified Svennerholm upper phase lipid extract, was determined to be 24% lower in the monophasic lipid extract when a sample concentration of 1.0 mg/ml retina tissue equivalent was analyzed (see supplementary Fig. IIIA). This observed difference in total ganglioside normalized abundance was abolished at a sample concentration of 0.5 mg/ml (see supplementary Fig. IIIB), consistent with the elimination of relative ion suppression at lower sample concentrations. However, the close agreement of the relative ganglioside class distributions obtained from each type of lipid extract when analyzed at a concentration of 1.0 mg/ml (Fig. 4A) implies that the difference in absolute ion intensities between the two extraction methods observed at this concentration does not alter the relative abundances of gangliosides under the experimental conditions employed, except for those at the lowest abundances (e.g., GM3 and GQ1). The summed abundances of individual ganglioside classes normalized to the abundance of the PC_(14:0/14:0) internal standard, expressed as the ratio of ganglioside class abundance to internal standard abundance at a sample concentration of 1.0 mg/ml retina tissue equivalents, is shown in supplementary Fig. IIIC. Compared with the modified Svennerholm upper phase, this ratio was 23.1 and 36.5% lower for GD3 and GT1 gangliosides, respectively, in the monophasic lipid extract. The summed abundances of GQ1 and GM3 gangliosides normalized to the internal standard were reduced 69.1 and 55.4%, respectively, in the monophasic lipid extract, although the large error associated with measurement of these low abundance classes prevented the difference from reaching statistical significance. This may indicate that relative ion suppression effects are observed to a greater extent for very low abundance lipids, and imply that subtle class-specific differences exist in the extent of ganglioside ion suppression at this sample concentration. Normalization of ganglioside species to internal standards of the same lipid class may theoretically overcome this phenomenon. However, this would require the introduction of a broad range of ganglioside standards to each sample, but such a strategy is currently hampered by the lack of availability of appropriate standards. Conversely, no observed differences in the summed abundances of each ganglioside class normalized to the abundance of the internal standard were observed between the modified Svennerholm and monophasic lipid extracts at a sample concentration of 0.5 mg/ml (supplementary Fig. IIID), consistent with supplementary Fig. IIIB. The standard

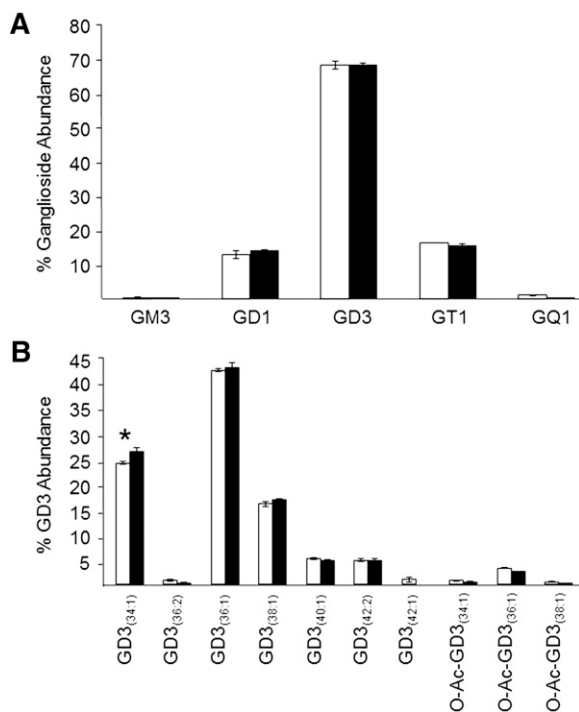


Fig. 4. A: Percent total ganglioside lipid abundance distributions of each observed ganglioside lipid class in the modified Svennerholm upper phase (open bars) and monophasic (filled bars) retina lipid extracts, as determined by negative ionization mode high-resolution ($R = 100,000$)/accurate MS and MS/MS analysis (sample concentration corresponding to 1.0 mg/ml of original retina tissue extracted). B: Percent ganglioside GD3 lipid abundance distributions of the individual ganglioside GD3 species in the modified Svennerholm upper phase (open bars) and monophasic (filled bars) retina lipid extract. Data represent the mean abundance \pm standard deviation from $n = 3$ separate lipid extracts. * $P < 0.05$.

deviations associated with measurement of ganglioside ion abundances in the monophasic lipid extract were smaller than those in the modified Svennerholm lipid extract, despite their lower absolute ion abundances, at this sample concentration. However, the measurement of the lowest abundance retinal gangliosides, GQ1 and GM3, became unfeasible in both the modified Svennerholm and monophasic lipid extracts at 0.5 mg/ml, as these species did not consistently exceed the limit of detection. Based on these results, we determined that a working sample concentration of 1.0 mg/ml retina tissue equivalents represented a suitable compromise between minimization of ion suppression and sensitivity of detection for low abundance lipid species.

A complete list of retinal ganglioside lipids detected in this study, from both the modified Svennerholm upper phase and monophasic lipid extraction approaches, is provided in **Table 1**. Overall, 26 ganglioside lipids were detected in the ganglioside-enriched modified Svennerholm upper phase extract, while all ganglioside species except the low abundance GD3_(42:1) lipid were also detected in the monophasic lipid extract. Given that the ganglioside abundances are expressed here as percent total ganglioside for each ganglioside class, and therefore interdependent on each other, the use of Student's *t*-test is not

appropriate for statistical analysis of this data. Therefore, we utilized the Sidak's multiple comparisons test to ensure a high power of analysis despite the small number of sample replicates in each group. Using this analysis method, statistically significant differences were observed in the relative abundances of several individual ganglioside species between the two extraction methods. However, the magnitude of these observed differences was generally small. Real differences in the mean abundances of several other ganglioside species were also observed. However these did not reach the level of statistical significance. The standard deviations for all except the least abundant of these already low abundance ganglioside lipids (e.g., the GM3 and GQ1 subclasses) were found to be similar in magnitude, albeit slightly higher, in the monophasic lipid extract compared with those in the modified Svennerholm upper phase. These overall small increases are likely due to the modest ion suppression effects described above for these low abundance lipids in the monophasic lipid extract.

Notably, each analysis was performed on a lipid extract corresponding to an amount of only ~10 µg of retinal tissue, following sample dilution. Taken together, these data support the use of a simple monophasic lipid extraction method in combination with direct infusion

TABLE 1. Retina ganglioside composition determined by two different lipid extraction methods

| Species | <i>m/z</i> | Molecular Ion | Ganglioside Abundance (%) | | <i>P</i> |
|----------------|------------|----------------------|---------------------------|---------------|--------------|
| | | | Upper Phase | Monophase | |
| GD3 | | | | | |
| GD3(34:1) | 720.8970 | [M-2H] ²⁻ | 24.09 ± 0.28 | 26.39 ± 0.90 | ^a |
| GD3(36:2) | 733.9048 | [M-2H] ²⁻ | 0.89 ± 0.17 | 0.33 ± 0.11 | ns |
| GD3(36:1) | 734.9126 | [M-2H] ²⁻ | 42.46 ± 0.29 | 43.01 ± 1.09 | ns |
| GD3(38:1) | 748.9283 | [M-2H] ²⁻ | 16.04 ± 0.48 | 16.86 ± 0.23 | ns |
| GD3(40:1) | 762.9439 | [M-2H] ²⁻ | 5.11 ± 0.22 | 4.66 ± 0.30 | ns |
| GD3(42:2) | 775.9517 | [M-2H] ²⁻ | 4.77 ± 0.31 | 4.75 ± 0.28 | ns |
| GD3(42:1) | 776.9596 | [M-2H] ²⁻ | 0.93 ± 0.57 | — | ns |
| O-Ac-GD3(34:1) | 741.9023 | [M-2H] ²⁻ | 0.77 ± 0.07 | 0.51 ± 0.10 | ns |
| O-Ac-GD3(36:1) | 755.9179 | [M-2H] ²⁻ | 3.23 ± 0.06 | 2.53 ± 0.10 | ns |
| O-Ac-GD3(38:1) | 769.9336 | [M-2H] ²⁻ | 0.52 ± 0.02 | 0.27 ± 0.01 | ns |
| GD1 | | | | | |
| GD1(34:1) | 903.4631 | [M-2H] ²⁻ | 0.33 ± 0.01 | 0.20 ± 0.34 | ns |
| GD1(36:1) | 917.4787 | [M-2H] ²⁻ | 55.52 ± 0.90 | 60.82 ± 2.53 | ^a |
| GD1(38:1) | 931.4944 | [M-2H] ²⁻ | 32.16 ± 1.06 | 32.25 ± 1.93 | ns |
| GD1(40:1) | 945.5100 | [M-2H] ²⁻ | 1.17 ± 0.12 | 1.29 ± 0.31 | ns |
| O-Ac-GD1(36:1) | 938.4840 | [M-2H] ²⁻ | 7.08 ± 0.22 | 3.73 ± 0.72 | ^a |
| O-Ac-GD1(38:1) | 952.4996 | [M-2H] ²⁻ | 3.74 ± 0.22 | 1.71 ± 0.21 | ns |
| GT1 | | | | | |
| GT1(36:1) | 1,063.0264 | [M-2H] ²⁻ | 39.27 ± 1.36 | 42.98 ± 1.31 | ^a |
| GT1(38:4) | 1,074.0186 | [M-2H] ²⁻ | 3.39 ± 0.66 | 5.02 ± 1.22 | ns |
| GT1(38:1) | 1,077.0421 | [M-2H] ²⁻ | 22.82 ± 0.99 | 21.73 ± 1.14 | ns |
| O-Ac-GT1(36:1) | 1,084.0317 | [M-2H] ²⁻ | 19.69 ± 0.37 | 19.02 ± 1.39 | ns |
| O-Ac-GT1(38:4) | 1,095.0239 | [M-2H] ²⁻ | 1.19 ± 0.56 | 1.06 ± 0.98 | ns |
| O-Ac-GT1(38:1) | 1,098.0473 | [M-2H] ²⁻ | 12.05 ± 0.32 | 8.81 ± 1.73 | ^a |
| GQ1 | | | | | |
| GQ1(36:1) | 1,208.5741 | [M-2H] ²⁻ | 34.30 ± 5.22 | 41.72 ± 21.86 | ns |
| O-Ac-GQ1(36:1) | 1,229.5794 | [M-2H] ²⁻ | 63.78 ± 4.65 | 54.62 ± 20.29 | ns |
| GM3 | | | | | |
| GM3(34:1) | 1,151.7058 | [M-H] ⁻ | 44.51 ± 5.40 | 60.49 ± 42.48 | ns |
| GM3(36:1) | 1,179.7371 | [M-H] ⁻ | 55.49 ± 5.40 | 39.5 ± 42.49 | ns |
| | | Total | 26 | 25 | |

Data are presented as mean ± standard deviation from n = 3 separate lipid extracts. Sample concentration: 1.0 mg/ml of original retina tissue extracted. O-Ac: *O*-acetylated headgroup; ns, not statistically significant.

^a*P* < 0.05.

nESI-high-resolution/accurate mass MS and MS/MS to enable analysis of relatively low abundance polar lipid classes such as gangliosides, when proper evaluation and control of sample preparation and analysis conditions has been employed.

Evaluation of retina phospholipid and low abundance nonpolar sphingolipid profiles from monophasic versus modified Folch lower phase lipid extracts

Given that the monophasic retina lipid extract was found, as expected, to contain significant levels of numerous polar and nonpolar phospholipid species in addition to the polar ganglioside lipids described above, we also evaluated the utility of the monophasic retina lipid extraction method for comprehensive lipidome analysis, compared with the conventional modified Folch retina lipid extract that is typical of the biphasic lipid extraction procedures used in most lipidomic analysis studies. In order to eliminate potential isobaric exact-mass overlap of PE and PS phospholipids with molecular species of other lipid classes, including PA, PC, and PG, respectively, as well as to resolve isobaric exact-mass overlap of 1-*O*-alkenyl ether (plasmalogen) lipids with unsaturated 1-*O*-alkyl ether lipids, we first subjected the monophasic and modified Folch lower phase retina lipid extracts to sequential functional group derivatization reactions with $^{13}\text{C}_1$ -DMBNHS followed by iodine and methanol, as previously described (6, 34). Next, the derivatized lipid extracts were subjected to serial dilution and analyzed by positive ionization mode nESI-high-resolution/accurate MS using the same strategy described in Fig. 3 in order to determine the dilution range for which detector response was linear, and where absolute and relative ion suppression was minimized. Similar to the negative ionization mode analysis results, dilutions resulting in sample concentrations ranging from 1 to 0.125 mg/ml of original retina tissue extracted were found to yield a linear response with respect to ion abundance

(data not shown). Importantly, as seen in the representative positive ionization mode high-resolution/accurate mass spectra in Fig. 5A and Fig. 5B, respectively, and by examining the distribution of individual PC and PE lipid species identified from these spectra (Fig. 6A and Fig. 6B, respectively), the relative distributions of lipids observed from the gold standard Folch lower phase lipid extract and the monophasic lipid extract were found to be virtually identical, and in both cases were in good agreement with previously published descriptions of rat retina phospholipid content by us and others (9, 15, 53). Minor differences in phospholipid molecular species distribution between this and previous studies of rat retina are most likely due to differences in the strains, ages, and diets of the rats used in the experiments. In the present study, the percent abundance of only two PC and one PE species were determined to be significantly different, albeit small, between the two extraction methods. Notably, however, higher absolute lipid ion abundances were observed in the monophasic extract for both PC and PE lipid classes, most likely due to the reduced sample handling steps compared with the Folch lower phase lipid extraction protocol, where isolation of the lower phase requires efficient exclusion of the interphase and upper phases. This is clearly shown in the insets to Fig. 6, where the total normalized abundances of all PC and PE lipids in the monophasic extract were determined to be 40.4 and 37.0% higher, respectively, than in the modified Folch lower phase.

Similarly, the monophasic retina lipid extraction method also yielded increased total normalized abundances for relatively low abundance nonpolar lipids, such as the sphingolipids Cer and SM. As shown in Fig. 7A, B, the relative distributions of these species were found to be identical from both extraction methods, with the total normalized abundances of all Cer species found to be significantly higher (47.2%) in the monophasic lipid extract than the modified Folch lipid extract, and the total normalized abundances of SM species also trending toward an increase

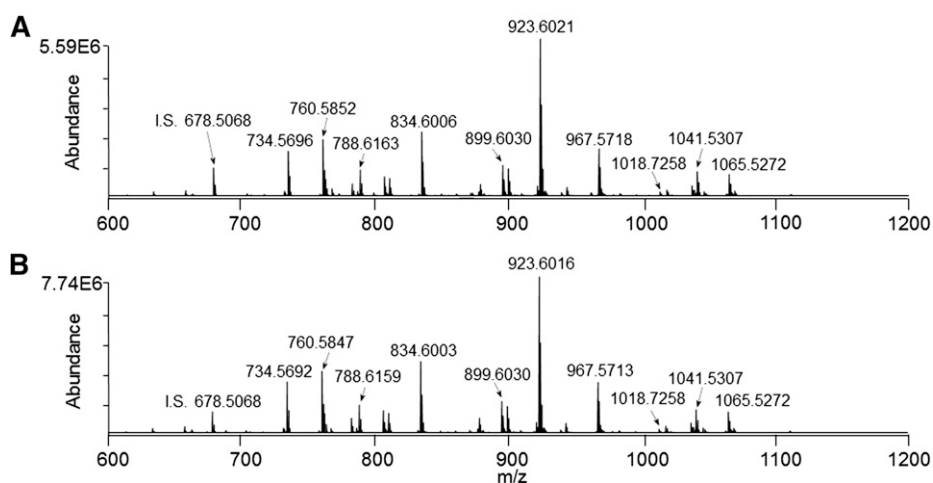


Fig. 5. Positive ionization mode high-resolution ($R = 100,000$)/accurate mass spectrum of a modified Folch lower phase retina lipid extract (A) and the monophasic retina lipid extract (B) after sequential functional group selective derivatization of PE, PS, and plasmalogen lipids (sample concentration corresponding to 1.0 mg/ml of original retina tissue extracted). I.S., internal standard. $\text{PC}_{(14:0/14:0)}$ (0.5 μM).

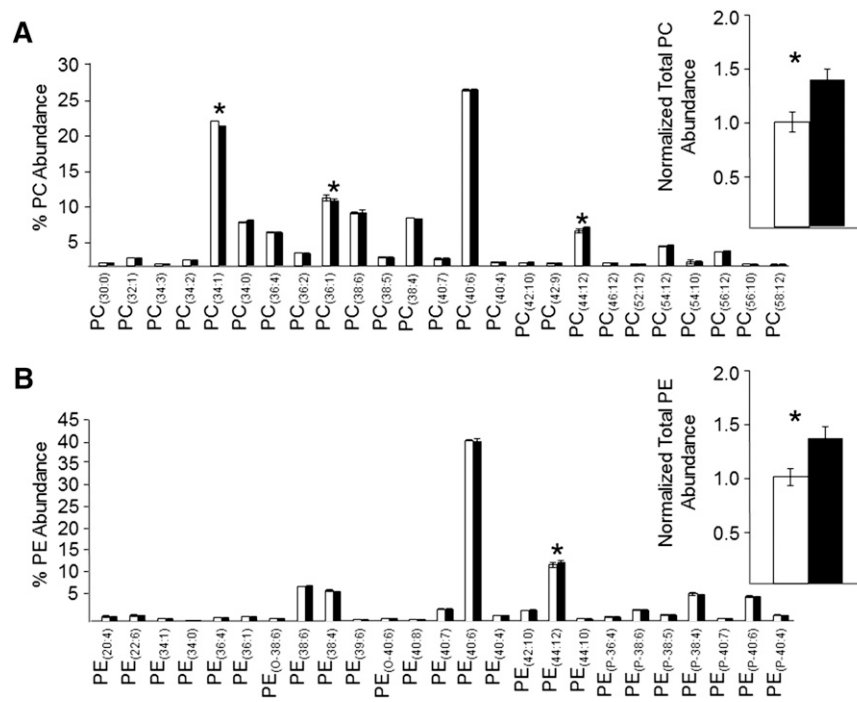


Fig. 6. Modified Folch lower phase (open bars) and monophasic (filled bars) retina lipid extracts (sample concentration corresponding to 1.0 mg/ml of original retina tissue extracted) were subjected to positive ionization mode high-resolution ($R = 100,000$)/accurate MS for quantitative comparison of individual PC lipid species as a percent of the total PC ion abundance (A) (inset: normalized ion abundances summed for all PC species) and individual PE molecular lipid species as a percent of the total PE ion abundance (B) (inset: normalized ion abundances summed for all PE species). Data represent the mean \pm standard deviation from $n = 3$ separate lipid extracts. * $P < 0.05$.

(26.4%), albeit not significant, consistent with that described above for the abundant phospholipid species. Moreover, the individual molecular species of SM and Cer were overall very similar to those observed in previous reports of

rat retina SM and Cer composition (53, 57), with any observed subtle differences in nonpolar sphingolipid species detected likely due to differences in the strains, ages, and diets of the rats used across these studies.

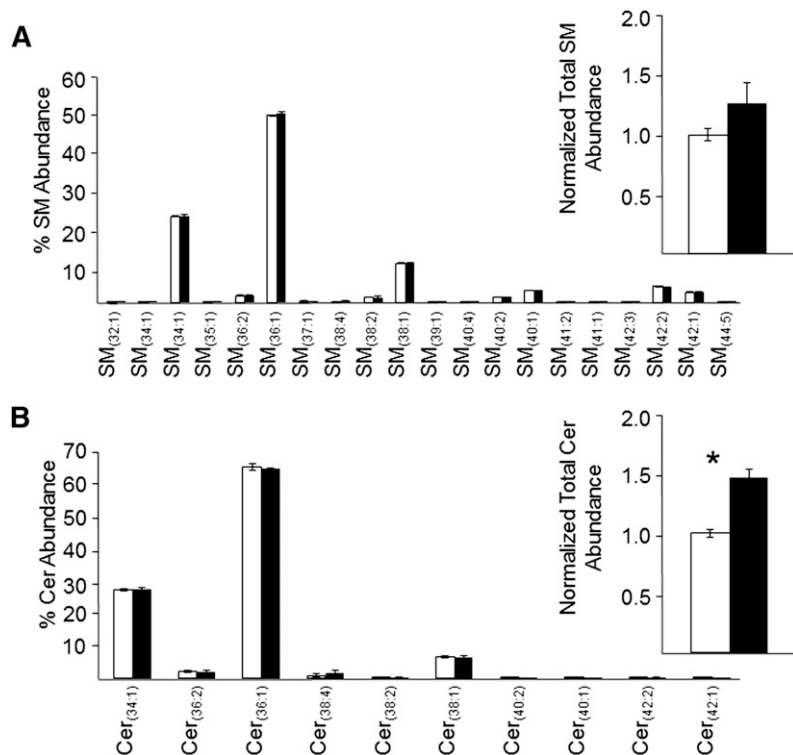



Fig. 7. Modified Folch lower phase (open bars) and monophasic (filled bars) retina lipid extracts (sample concentration corresponding to 1.0 mg/ml of original retina tissue extracted) were subjected to positive ionization mode high-resolution ($R = 100,000$)/accurate MS for quantitative comparison of individual SM lipid species as a percent of the total SM ion abundance (A) (inset: normalized ion abundances summed for all SM species) and individual Cer lipid species as a percent of the total Cer ion abundance (B) (inset: normalized ion abundances summed for all Cer species). Data represent the mean \pm standard deviation from $n = 3$ separate lipid extracts. * $P < 0.05$.

These data clearly demonstrate that the monophasic lipid extraction approach provides essentially identical coverage and distributions of phospholipid and low abundance non-polar sphingolipid species compared with those observed from a typically employed biphasic lipid extraction method, but with increased detection sensitivity and decreased technical variance due to decreased sample handling and elimination of analyte losses during phase partitioning.

CONCLUSIONS

Lipid extraction of biological samples using a monophasic methanol/chloroform/water mixture, coupled with direct infusion shotgun nESI-high-resolution/accurate MS analysis, provides a viable strategy for the simultaneous observation of both low and high abundance lipids, regardless of polarity. Despite the presence of modest relative ion suppression effects resulting from the mixture complexity and presence of abundant phospholipids, careful appraisal of sample preparation and analysis conditions (i.e., working within the linear concentration range of detector response for the samples of interest) enables the effective use of monophasic lipid extraction for the evaluation of rat retina ganglioside content. Similar determination of absolute and relative ion suppression effects should be performed for lipid extracts from different types of tissue or cells, and when comparing samples that undergo significant changes in lipid composition and abundances between control and treatment groups, as the extent of ion suppression may be greater in one tissue or treatment type than another. In these cases, sample concentrations should be appropriately normalized (e.g., by dilution) to the same total lipid abundances prior to performing quantitative analysis. While lipid extraction methods designed for the specific extraction of gangliosides, such as modified the Svennerholm methods, may provide advantages over a monophasic extraction system for the analysis of extremely low abundance polar lipid species, the monophasic extraction protocol described here enables lipidomic analysis of a majority of the retinal gangliosides that are present in the modified Svennerholm extract upper phase, with similar distributions and only minor increased variance in abundances.

Moreover, the monophasic retinal lipid extraction protocol enables the acquisition of retinal phospholipid and nonpolar sphingolipid profiles that are very similar to those obtained from a modified Folch biphasic lipid extraction method, but with the benefits of significantly improved sensitivity and reduced technical variance. Therefore, the monophasic lipid extraction method is recommended for the lipidome analysis of samples where lipid classes and subclasses covering a broad range of polarity and structural heterogeneity are of interest, while specialized lipid extractions should optimally be employed when the analysis of only a narrowly defined subset of extremely low abundance lipids is desired. In this study, rat retina ganglioside, nonpolar sphingolipid, and phospholipid profiles were obtained from the equivalent of only 10 μg of retinal tissue. Therefore, the use of the described

monophasic lipid extraction procedure in combination with lipid functional group-specific derivatization and direct infusion high-resolution/accurate MS enables shotgun lipid analysis of highly polar and nonpolar lipid classes of disparate abundances from minute amounts of biological samples, facilitating the attainment of more inclusive and comprehensive lipidomic studies. 

The authors thank Ms. Kristen Reese for acquiring preliminary data associated with this study.

REFERENCES

1. Cao, G., R. J. Konrad, S. D. Li, and C. Hammond. 2012. Glycerolipid acyltransferases in triglyceride metabolism and energy homeostasis-potential as drug targets. *Endocr. Metab. Immune Disord. Drug Targets*. **12**: 197–206.
2. Li, M., L. Yang, Y. Bai, and H. Liu. 2014. Analytical methods in lipidomics and their applications. *Anal. Chem.* **86**: 161–175.
3. Han, X., K. Yang, and R. W. Gross. 2012. Multi-dimensional mass spectrometry-based shotgun lipidomics and novel strategies for lipidomic analyses. *Mass Spectrom. Rev.* **31**: 134–178.
4. Shui, G., J. W. Stebbins, B. D. Lam, W. F. Cheong, S. M. Lam, F. Gregoire, J. Kusunoki, and M. R. Wenk. 2011. Comparative plasma lipidome between human and cynomolgus monkey: are plasma polar lipids good biomarkers for diabetic monkeys? *PLoS ONE*. **6**: e19731.
5. Hopperton, K. E., R. E. Duncan, R. P. Bazinet, and M. C. Archer. 2014. Fatty acid synthase plays a role in cancer metabolism beyond providing fatty acids for phospholipid synthesis or sustaining elevations in glycolytic activity. *Exp. Cell Res.* **320**: 302–310.
6. Phaner, C. J., S. Liu, H. Ji, R. J. Simpson, and G. E. Reid. 2012. Comprehensive lipidome profiling of isogenic primary and metastatic colon adenocarcinoma cell lines. *Anal. Chem.* **84**: 8917–8926.
7. Cheng, H., M. Wang, J. L. Li, N. J. Cairns, and X. Han. 2013. Specific changes of sulfatide levels in individuals with pre-clinical Alzheimer's disease: an early event in disease pathogenesis. *J. Neurochem.* **127**: 733–738.
8. Tikhonenko, M., T. A. Lydic, Y. Wang, W. Chen, M. Opreanu, A. Sochacki, K. M. McSorley, R. L. Renis, T. Kern, D. B. Jump, et al. 2010. Remodeling of retinal fatty acids in an animal model of diabetes: a decrease in long-chain polyunsaturated fatty acids is associated with a decrease in fatty acid elongases Elovl2 and Elovl4. *Diabetes*. **59**: 219–227.
9. Lydic, T. A., R. Renis, J. V. Busik, and G. E. Reid. 2009. Analysis of retina and erythrocyte glycerophospholipid alterations in a rat model of type 1 diabetes. *JALA Charlottesv. Va.* **14**: 383–399.
10. Opreanu, M., M. Tikhonenko, S. Bozack, T. A. Lydic, G. E. Reid, K. M. McSorley, A. Sochacki, G. I. Perez, W. J. Esselman, T. Kern, et al. 2011. The unconventional role of acid sphingomyelinase in regulation of retinal microangiopathy in diabetic human and animal models. *Diabetes*. **60**: 2370–2378.
11. Tikhonenko, M., T. A. Lydic, M. Opreanu, S. Li Calzi, S. Bozack, K. M. McSorley, A. L. Sochacki, M. S. Faber, S. Hazra, S. Duclos, et al. 2013. N-3 polyunsaturated fatty acids prevent diabetic retinopathy by inhibition of retinal vascular damage and enhanced endothelial progenitor cell reparative function. *PLoS ONE*. **8**: e55177.
12. Fox, T. E., X. Han, S. Kelly, A. H. Merrill, R. E. Martin, R. E. Anderson, T. W. Gardner, and M. Kester. 2006. Diabetes alters sphingolipid metabolism in the retina: a potential mechanism of cell death in diabetic retinopathy. *Diabetes*. **55**: 3573–3580.
13. Agbaga, M. P., R. S. Brush, M. N. Mandal, K. Henry, M. H. Elliott, and R. E. Anderson. 2008. Role of Stargardt-3 macular dystrophy protein (ELOVL4) in the biosynthesis of very long chain fatty acids. *Proc. Natl. Acad. Sci. USA*. **105**: 12843–12848.
14. SanGiovanni, J. P., E. Y. Chew, T. E. Clemons, M. D. Davis, F. L. Ferris, G. R. Gensler, N. Kurinij, A. S. Lindblad, R. C. Milton, J. M. Seddon, et al. 2007. The relationship of dietary lipid intake and age-related macular degeneration in a case-control study: AREDS Report No. 20. *Arch. Ophthalmol.* **125**: 671–679.
15. Ford, D. A., J. K. Monda, R. S. Brush, R. E. Anderson, M. J. Richards, and S. J. Fliesler. 2008. Lipidomic analysis of the retina in a rat model of Smith-Lemli-Opitz syndrome: alterations in docosahexaenoic

- acid content of phospholipid molecular species. *J. Neurochem.* **105**: 1032–1047.
16. Connor, K. M., J. P. SanGiovanni, C. Lofqvist, C. M. Aderman, J. Chen, A. Higuchi, S. Hong, E. A. Pravda, S. Majchrzak, D. Carper, et al. 2007. Increased dietary intake of omega-3-polyunsaturated fatty acids reduces pathological retinal angiogenesis. *Nat. Med.* **13**: 868–873.
 17. Svennerholm, L., and P. Fredman. 1980. A procedure for the quantitative isolation of brain gangliosides. *Biochim. Biophys. Acta.* **617**: 97–109.
 18. Merrill, A. H., M. C. Sullards, J. C. Allegood, S. Kelly, and E. Wang. 2005. Sphingolipidomics: high-throughput, structure-specific, and quantitative analysis of sphingolipids by liquid chromatography tandem mass spectrometry. *Methods.* **36**: 207–224.
 19. Milne, S. B., P. T. Ivanova, D. DeCamp, R. C. Hsueh, and H. A. Brown. 2005. A targeted mass spectrometric analysis of phosphatidylinositol phosphate species. *J. Lipid Res.* **46**: 1796–1802.
 20. Merrill, A. H., Jr. 2011. Sphingolipid and glycosphingolipid metabolic pathways in the era of sphingolipidomics. *Chem. Rev.* **111**: 6387–6422.
 21. Li, J., M. Hoene, X. Zhao, S. Chen, H. Wei, H. U. Haring, X. Lin, Z. Zeng, C. Weigert, R. Lehmann, et al. 2013. Stable isotope-assisted lipidomics combined with nontargeted isotopomer filtering, a tool to unravel the complex dynamics of lipid metabolism. *Anal. Chem.* **85**: 4651–4657.
 22. Murphy, R. C., P. F. James, A. M. McAnoy, J. Krank, E. Duchoslav, and R. M. Barkley. 2007. Detection of the abundance of diacylglycerol and triacylglycerol molecular species in cells using neutral loss mass spectrometry. *Anal. Biochem.* **366**: 59–70.
 23. Ikeda, K., T. Shimizu, and R. Taguchi. 2008. Targeted analysis of ganglioside and sulfatide molecular species by LC/ESI-MS/MS with theoretically expanded multiple reaction monitoring. *J. Lipid Res.* **49**: 2678–2689.
 24. Sato, A., K. Dodo, M. Makishima, Y. Hashimoto, and M. Sodeoka. 2013. Synthesis and evaluation of 2,3-dinorprostaglandins: Dinor-PGD1 and 13-epi-dinor-PGD1 are peroxisome proliferator-activated receptor alpha/gamma dual agonists. *Bioorg. Med. Chem. Lett.* **23**: 3013–3017.
 25. Fox, T. E., M. C. Bewley, K. A. Unrath, M. M. Pedersen, R. E. Anderson, D. Y. Jung, L. S. Jefferson, J. K. Kim, S. K. Bronson, J. M. Flanagan, et al. 2011. Circulating sphingolipid biomarkers in models of type 1 diabetes. *J. Lipid Res.* **52**: 509–517.
 26. Quehenberger, O., A. M. Armando, A. H. Brown, S. B. Milne, D. S. Myers, A. H. Merrill, S. Bandyopadhyay, K. N. Jones, S. Kelly, R. L. Shaner, et al. 2010. Lipidomics reveals a remarkable diversity of lipids in human plasma. *J. Lipid Res.* **51**: 3299–3305.
 27. Heiskanen, L. A., M. Suoniemi, H. X. Ta, K. Tarasov, and K. Ekroos. 2013. Long-term performance and stability of molecular shotgun lipidomic analysis of human plasma samples. *Anal. Chem.* **85**: 8757–8763.
 28. Han, X., and R. W. Gross. 2005. Shotgun lipidomics: multidimensional MS analysis of cellular lipidomes. *Expert Rev. Proteomics.* **2**: 253–264.
 29. Ekroos, K., M. Janis, K. Tarasov, R. Hurme, and R. Laaksonen. 2010. Lipidomics: a tool for studies of atherosclerosis. *Curr. Atheroscler. Rep.* **12**: 273–281.
 30. Brown, S. H., C. M. Kunnen, E. Duchoslav, N. K. Dolla, M. J. Kelso, E. B. Papas, P. Lazon de la Jara, M. D. Willcox, S. J. Blanksby, and T. W. Mitchell. 2013. A comparison of patient matched meibum and tear lipidomes. *Invest. Ophthalmol. Vis. Sci.* **54**: 7417–7424.
 31. Han, X., K. Yang, and R. W. Gross. 2008. Microfluidics-based electrospray ionization enhances the intrasource separation of lipid classes and extends identification of individual molecular species through multi-dimensional mass spectrometry: development of an automated high-throughput platform for shotgun lipidomics. *Rapid Commun. Mass Spectrom.* **22**: 2115–2124.
 32. Ejsing, C. S., J. L. Sampaio, V. Surendranath, E. Duchoslav, K. Ekroos, R. W. Klemm, K. Simons, and A. Shevchenko. 2009. Global analysis of the yeast lipidome by quantitative shotgun mass spectrometry. *Proc. Natl. Acad. Sci. USA.* **106**: 2136–2141.
 33. Dennis, E. A., R. A. Deems, R. Harkewicz, O. Quehenberger, H. A. Brown, S. B. Milne, D. S. Myers, C. K. Glass, G. Hardiman, D. Reichart, et al. 2010. A mouse macrophage lipidome. *J. Biol. Chem.* **285**: 39976–39985.
 34. Fhaner, C. J., S. Liu, X. Zhou, and G. E. Reid. 2013. Functional group selective derivatization and gas-phase fragmentation reactions of plasmalogen glycerophospholipids. *Mass Spectrom. (Tokyo)*. **2**: S0015.
 35. Lydic, T. A., J. V. Busik, W. J. Esselman, and G. E. Reid. 2009. Complementary precursor ion and neutral loss scan mode tandem mass spectrometry for the analysis of glycerophosphatidylethanolamine lipids from whole rat retina. *Anal. Bioanal. Chem.* **394**: 267–275.
 36. Schuhmann, K., R. Almeida, M. Baumert, R. Herzog, S. R. Bornstein, and A. Shevchenko. 2012. Shotgun lipidomics on a LTQ Orbitrap mass spectrometer by successive switching between acquisition polarity modes. *J. Mass Spectrom.* **47**: 96–104.
 37. Han, X., and R. W. Gross. 2005. Shotgun lipidomics: electrospray ionization mass spectrometric analysis and quantitation of cellular lipidomes directly from crude extracts of biological samples. *Mass Spectrom. Rev.* **24**: 367–412.
 38. Folch, J., M. Lees, and G. H. Sloane Stanley. 1957. A simple method for the isolation and purification of total lipides from animal tissues. *J. Biol. Chem.* **226**: 497–509.
 39. Matyash, V., G. Liebisch, T. V. Kurzchalia, A. Shevchenko, and D. Schwudke. 2008. Lipid extraction by methyl-tert-butyl ether for high-throughput lipidomics. *J. Lipid Res.* **49**: 1137–1146.
 40. Mukherjee, P., A. C. Faber, L. M. Shelton, R. C. Baek, T. C. Chiles, and T. N. Seyfried. 2008. Thematic review series: sphingolipids. Ganglioside GM3 suppresses the proangiogenic effects of vascular endothelial growth factor and ganglioside GD1a. *J. Lipid Res.* **49**: 929–938.
 41. Wijesinghe, D. S., J. C. Allegood, L. B. Gentile, T. E. Fox, M. Kester, and C. E. Chalfant. 2010. Use of high performance liquid chromatography-electrospray ionization-tandem mass spectrometry for the analysis of ceramide-1-phosphate levels. *J. Lipid Res.* **51**: 641–651.
 42. Sekino-Suzuki, N., K. Yuyama, T. Miki, M. Kaneda, H. Suzuki, N. Yamamoto, T. Yamamoto, C. Oneyama, M. Okada, and K. Kasahara. 2013. Involvement of gangliosides in the process of Cbp/PAG phosphorylation by Lyn in developing cerebellar growth cones. *J. Neurochem.* **124**: 514–522.
 43. Malisan, F., L. Franchi, B. Tomassini, N. Ventura, I. Condo, M. R. Rippon, A. Rufini, L. Liberati, C. Nachtigall, B. Kniep, et al. 2002. Acetylation suppresses the proapoptotic activity of GD3 ganglioside. *J. Exp. Med.* **196**: 1535–1541.
 44. Malisan, F., and R. Testi. 2002. GD3 ganglioside and apoptosis. *Biochim. Biophys. Acta.* **1585**: 179–187.
 45. Chung, T. W., S. J. Kim, H. J. Choi, K. J. Kim, M. J. Kim, S. H. Kim, H. J. Lee, J. H. Ko, Y. C. Lee, A. Suzuki, et al. 2009. Ganglioside GM3 inhibits VEGF/VEGFR-2-mediated angiogenesis: direct interaction of GM3 with VEGFR-2. *Glycobiology.* **19**: 229–239.
 46. Liu, Y., J. McCarthy, and S. Ladisch. 2006. Membrane ganglioside enrichment lowers the threshold for vascular endothelial cell angiogenic signaling. *Cancer Res.* **66**: 10408–10414.
 47. Kabayama, K., T. Sato, K. Saito, N. Loberto, A. Prinetti, S. Sonnino, M. Kinjo, Y. Igarashi, and J. Inokuchi. 2007. Dissociation of the insulin receptor and caveolin-1 complex by ganglioside GM3 in the state of insulin resistance. *Proc. Natl. Acad. Sci. USA.* **104**: 13678–13683.
 48. Nimrichter, L., M. M. Burdick, K. Aoki, W. Laroy, M. A. Fierro, S. A. Hudson, C. E. Von Seggern, R. J. Cotter, B. S. Bochner, M. Tiemeyer, et al. 2008. E-selectin receptors on human leukocytes. *Blood.* **112**: 3744–3752.
 49. Fong, B., C. Norris, E. Lowe, and P. McJarrow. 2009. Liquid chromatography-high-resolution mass spectrometry for quantitative analysis of gangliosides. *Lipids.* **44**: 867–874.
 50. Metelmann, W., Z. Vukelic, and J. Peter-Katalinic. 2001. Nano-electrospray ionization time-of-flight mass spectrometry of gangliosides from human brain tissue. *J. Mass Spectrom.* **36**: 21–29.
 51. Schiopu, C., C. Flangea, F. Capitan, A. Serb, Z. Vukelic, S. Kalanj-Bognar, E. Sisu, M. Przybylski, and A. D. Zamfir. 2009. Determination of ganglioside composition and structure in human brain hemangioma by chip-based nano-electrospray ionization tandem mass spectrometry. *Anal. Bioanal. Chem.* **395**: 2465–2477.
 52. Zamfir, A. D., D. Fabris, F. Capitan, C. Munteanu, Z. Vukelic, and C. Flangea. 2013. Profiling and sequence analysis of gangliosides in human astrocytoma by high-resolution mass spectrometry. *Anal. Bioanal. Chem.* **405**: 7321–7335.
 53. Busik, J. V., G. E. Reid, and T. A. Lydic. 2009. Global analysis of retina lipids by complementary precursor ion and neutral loss mode tandem mass spectrometry. *Methods Mol. Biol.* **579**: 33–70.
 54. Koivusalo, M., P. Haimi, L. Heikinheimo, R. Kostainen, and P. Somerharju. 2001. Quantitative determination of phospholipid compositions by ESI-MS: effects of acyl chain length, unsaturation, and lipid concentration on instrument response. *J. Lipid Res.* **42**: 663–672.
 55. Cech, N. B., and C. G. Enke. 2001. Practical implications of some recent studies in electrospray ionization fundamentals. *Mass Spectrom. Rev.* **20**: 362–387.
 56. O'Brien, J. P., and J. S. Brodbelt. 2013. Structural characterization of gangliosides and glycolipids via ultraviolet photodissociation mass spectrometry. *Anal. Chem.* **85**: 10399–10407.
 57. Chen, H., J. T. Tran, A. Eckerl, T. P. Huynh, M. H. Elliott, R. S. Brush, and N. A. Mandal. 2013. Inhibition of de novo ceramide biosynthesis by FTY720 protects rat retina from light-induced degeneration. *J. Lipid Res.* **54**: 1616–1629.